Eur. Phys. J. Plus (2017) **132**: 65
DOI 10.1140/epjp/i2017-11324-1

THE EUROPEAN PHYSICAL JOURNAL PLUS

Regular Article

Numerical investigation of the heat transfer of a ferrofluid inside a tube in the presence of a non-uniform magnetic field

Saman Hariri[1], Mojtaba Mokhtari[2], M. Barzegar Gerdroodbary[3], and Keivan Fallah[4,a]

[1] Department of Chemical Engineering, Iran University of Science &Technology, Tehran, Iran
[2] Department of Chemical & Petroleum Engineering, Sharif University of Technology, Tehran, Iran
[3] Department of Mechanical Engineering, Babol University of Technology, Babol, Iran
[4] Department of Mechanical Engineering, Sari Branch, Islamic Azad University, Sari, Iran

Received: 2 November 2016 / Revised: 6 December 2016
Published online: 10 February 2017 –

Abstract. In this article, a three-dimensional numerical investigation is performed to study the effect of a magnetic field on a ferrofluid inside a tube. This study comprehensively analyzes the influence of a non-uniform magnetic field in the heat transfer of a tube while a ferrofluid (water with 0.86 vol% nanoparticles (Fe_3O_4)) is let flow. The SIMPLEC algorithm is used for obtaining the flow and heat transfer inside the tube. The influence of various parameters, such as concentration of nanoparticles, intensity of the magnetic field, wire distance and Reynolds number, on the heat transfer is investigated. According to the obtained results, the presence of a non-uniform magnetic field significantly increases the Nusselt number (more than 300%) inside the tube. Also, the magnetic field induced by the parallel wire affects the average velocity of the ferrofluid and forms two strong eddies in the tube. Our findings show that the diffusion also raises as the concentration of the nanoparticle is increased.

Nomenclature

(a, b, c)	Center of the magnetic wire (m)
C_{p}	Specific heat (J kg^{-1} K^{-1})
D	Hydraulic diameter (m)
d_p	Magnetic particle diameter (m)
H_r	Characteristic magnetic field strength (A m^{-1})
H_x	Magnetic field intensity component in the x-direction (A m^{-1})
H_y	Magnetic field intensity component in the y-direction (A m^{-1})
H_z	Magnetic field intensity component in the z-direction (A m^{-1})
I	Electric intensity (A)
k	Thermal conductivity (W m^{-1} °C^{-1})
k_B	Boltzmann constant ($1.3806503 \times 10^{-23}$ JK^{-1})
M	Magnetization (A m^{-1})
Mn	Magnetic number
m_p	Particle magnetic moment (A m^2)
Nu	Nusselt number
q	Wall heat flux (W m^{-2})
Re	Reynolds number
T	Temperature (°C)

Greek symbols

φ	Volume fraction of particles
μ	Dynamic viscosity (N s m^{-2})
μ_0	Magnetic permeability in vacuum ($4\pi \times 10^{-7}$ TA m^{-1})
μ_B	Bohr magneton (9.27×10^{-24} A m^2)
ρ	Density (kg m^{-3})
σ	Electrical conductivity

Subscripts

avg	Average
f	Pertaining to base fluid
p	Pertaining to magnetic particles
η_{nf}	Nanofluid
0	Pertaining to inlet conditions

[a] e-mail: keivan.fallah@gmail.com (corresponding author)

1 Introduction

Efficient heat transfer in tubes is crucial in the performance of these instruments in various areas, such as cooling systems of micro devices, heat recovery systems, process plants, refrigeration, etc. Nanofluids, which are colloidal suspensions of nanoparticles inside the main fluid, significantly influence the heat transfer due to their improved thermal characteristics. Since ferrofluids contains magnetic particles, their characteristics are highly changed in the presence of a magnetic field.

A vast amount of research has been conducted on the heat transfer of a nanofluid inside various geometries in the last decade [1–3]. Mahanthesh *et al.* [2] studied heat and mass transfer effects on the mixed convective flow of a chemically reacting nanofluid past a moving/stationary vertical plate. Kadhim Hussein *et al.* [3] presented magneto-hydrodynamic natural convection in an inclined T-shaped enclosure for different nanofluids and subjected to a uniform heat source.

Wen *et al.* [4] reviewed several articles on various nanofluids for heat transfer applications. They presented a critical review of research on heat transfer applications of nanofluids with the aim of identifying the limiting factor so as to push forward their further development. Behroyan *et al.* [5] presented a comprehensive comparison of various CFD models for convective heat transfer of an Al_2O_3 nanofluid inside a heated tube. Their results indicated that the non-Newtonian single-phase model predicts more accurately the Nusselt number than the Newtonian single-phase model. Sheikholeslami *et al.* [6] reported the impact of inconstant magnetic field on forced convection. They illustrated that higher lid velocity has more sensible Kelvin forces effect. Zhao *et al.* [7] performed numerical investigations of laminar heat transfer and flow performance of Al_2O_3-water nanofluids in a flat tube. Their results showed that, compared to the tube flattening, nanoparticle volume concentration has a slight effect on the relative thermal-hydraulic performance between flat tubes and circular tube.

The numerical simulation of magnetic nanoparticles has been studied as a means to modify or enhance heat transfer on various applications and devices. Recently, scientists and researchers used CFD devices for simulation and evaluation of the non-uniform magnetic field on the heat transfer of magnetic nanoparticles [8–19]. Sheikholeslami and Ganji [8] studied the MHD Fe_3O_4-water heat transfer in an enclosure with moving and wavy walls. Mousavi *et al.* [9,10] presented numerical studies about the influence of the magnetic field on the heat transfer of a magnetic nanofluid in a sinusoidal double-pipe heat exchanger. Their simulations showed that the diffusion also elevates as the intensity of the magnetic field is increased.

Sheikholeslami and Ganji [11] reviewed the nanofluid convective heat transfer using semi analytical and numerical approaches in more than 100 references. Kim *et al.* [12] analyzed convective heat transfer characteristics of nanofluids under laminar and turbulent flow conditions. They found that the enhancement of the convective heat transfer was much higher than that of the thermal conductivity in comparison with thermal conductivity and convection of nanofluids. Also, the free convection of a magnetic nanofluid considering MFD viscosity effects was studied by Sheikholeslami *et al.* [13]. They found that reduction of the Nusselt number due to the MFD viscosity effect is more sensible for high Rayleigh number and low Hartmann number. Abdollahi *et al.* [14,15] also investigated the magnetic field effect on the pool boiling heat transfer of a ferrofluid. In other works, numerical simulation of heat transfer and flow separation of Al_2O_3/nanofluid in concentric annular pipes was investigated by Togun *et al.* [16]. They explained that increasing the nanoparticles of the Al_2O_3/nanofluid tends to enhance the heat transfer coefficient due to the nanoparticle heat transport in the base fluid which raises the convection heat transfer. Numerical investigation of a forced convective heat transfer of a Fe_3O_4-water nanofluid in the presence of an external magnetic source was done by Sheikholeslami *et al.* [17]. They found that heat transfer improvement increases with an increase in the Reynolds number but it reduces with an increase in the Hartmann number.

Furthermore, a numerical analysis of the nanofluid flow conveying nanoparticles through expanding and contracting gaps between permeable walls is explained by Hatami *et al.* [18]. This results showed that the velocity boundary layer thickness near the walls decreases with an increase in the Reynolds number and nanoparticle volume friction. Sheikholeslami [19] simulated a nanofluid spraying on an inclined rotating disk for cooling process. Their findings showed that the Nusselt number is an increasing function of each active parameter. Forced convection and pressure drop of a Fe_3O_4 nanofluid under an external magnetic field were investigated experimentally by Goharkhah *et al.* [20]. They showed that the rise of the pressure drop is an unavoidable effect of applying a magnetic field to the ferrofluid.

The main purpose of the present work is to investigate the influence of a magnetic field on the laminar convective heat transfer of magnetite nanofluids in a tube. The finite volume approach is applied to simulate the flow feature and obtain heat transfer inside the tube when the wire as the source of the non-uniform magnetic field is present. Various arrangements of the magnetic field (perpendicular and parallel to the flow) are investigated in this work. In addition, different intensities of the magnetic field are simulated to investigate their influence on the heat transfer along the pipe. Also, various concentrations of Fe_3O_4 in nanofluids are examined and the effects of inlet velocity on the temperature and convection performance of surfaces are discussed. Finally, the influence of the wire distance to the tube on the heat transfer rate of various nanofluids is compared.

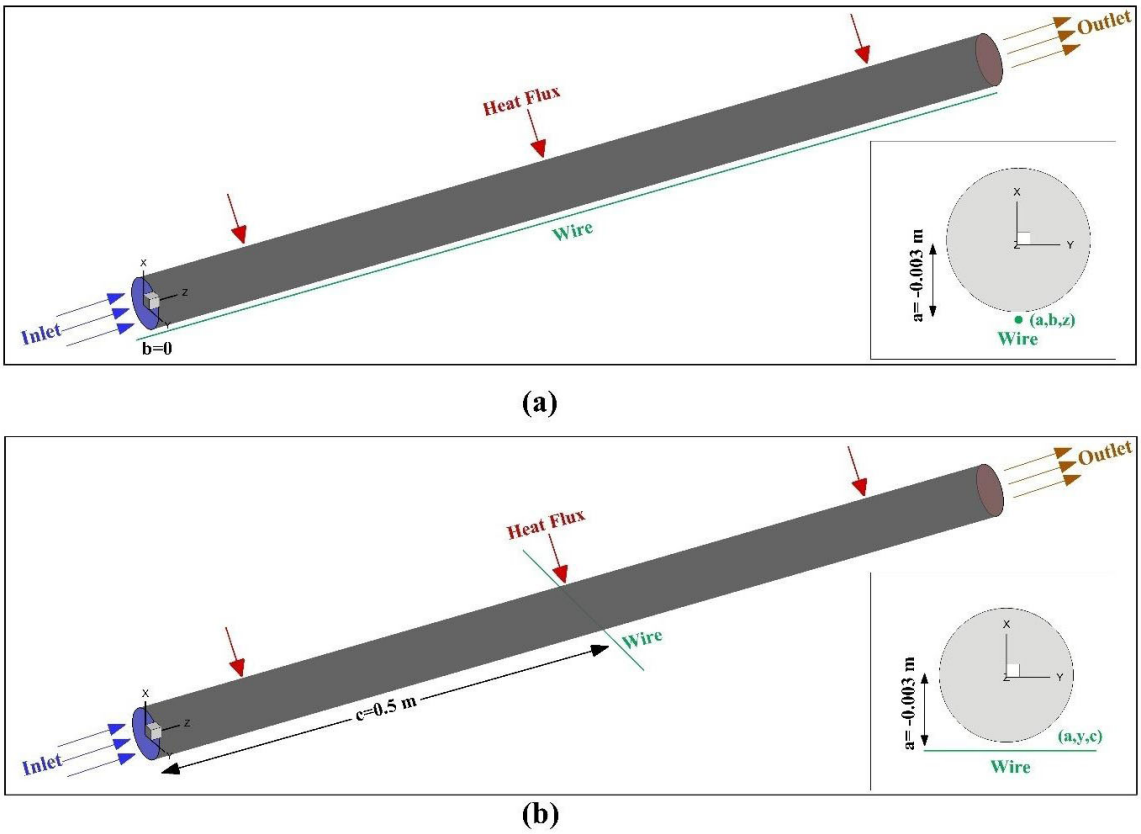

Fig. 1. Schematic and geometry of the tube with two different wire orientations: (a) parallel and (b) perpendicular to the tube.

2 Theoretical formulation

2.1 Geometry and grid

Figure 1 illustrates the three-dimensional schematic of the tube with the wire parallel and perpendicular to the axis of the tube. As an electric current goes through the wire, the magnetic field is generated in the direction of the x- and y-axis for the parallel wire (fig. 1(a)) and of the x- and z-axis for the perpendicular wire (fig. 1(b)).

Figure 2 illustrates the grid of a geometry with length $L = 1\,\mathrm{m}$ and the height of the inner tube $d_\mathrm{i} = 0.00554\,\mathrm{m}$. In the current study, three different grids with 870000, 1282000 and 1840000 elements are chosen as coarse, fine and very fine grids for the grid independency analysis, respectively. Figure 3 compares the Nusselt number of these grids along the axis of the tube with experimental results [21]. The plot clearly shows that the fine and very fine grids present reasonable results and the discrepancy with experimental data is less than 5%. Therefore, the fine grid is chosen for the further investigations.

2.2 Governing equations and numerical methods

In this paper, energy equations are coupled with Navier-Stokes equations to calculate the heat transfer rate of the nanofluid in a tube. It is assumed that the nanofluid is exposed to a magnetic field, so the components of the magnetic field should be taken into account in the momentum and energy equations as source terms. In addition, it is supposed that the effects of magnetic fields on the properties of the nanofluid are insignificant, and the Lorentz force is also considered to be negligible in the momentum equations compared to the magnetic force due to the electrical conductivity. With these assumptions, the conservation equations for the laminar steady state flow are as follows.

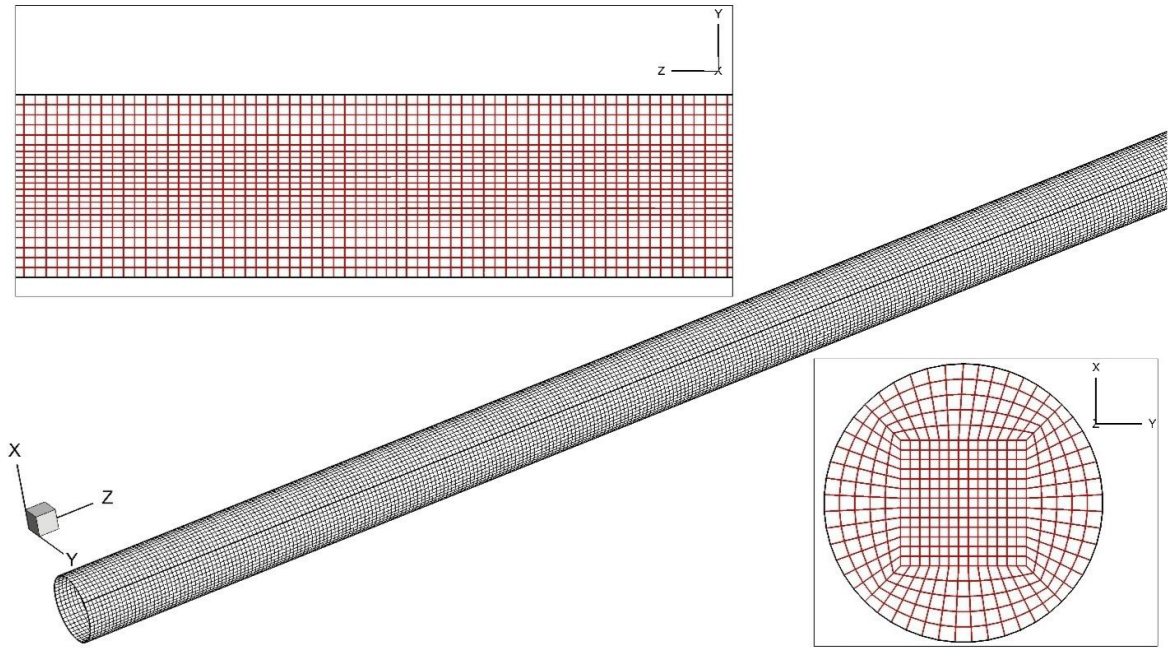

Fig. 2. Grid of domain.

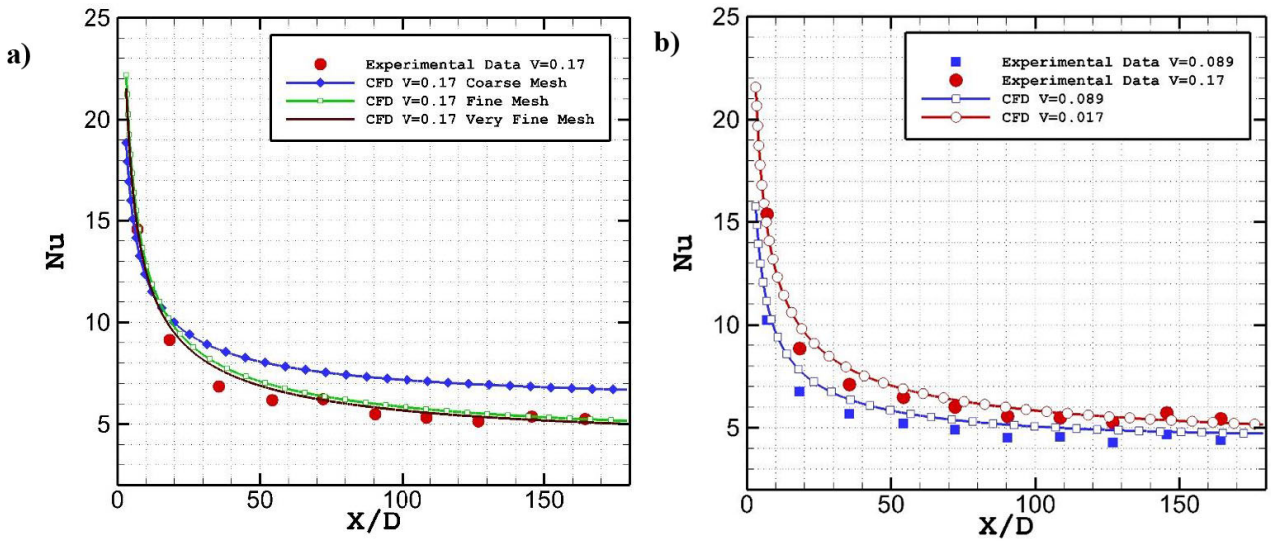

Fig. 3. Verification: (a) grid independency for water flow; (b) validation for ferrofluid.

Momentum equation:

$$\rho_{\mathrm{nf}}\left(u\frac{\partial u}{\partial x}+v\frac{\partial u}{\partial y}+w\frac{\partial u}{\partial z}\right)=-\frac{\partial p}{\partial x}+\mu_{\mathrm{nf}}\left(\frac{\partial^2 u}{\partial x^2}+\frac{\partial^2 u}{\partial y^2}+\frac{\partial^2 u}{\partial z^2}\right)+S_F(x) \tag{1}$$

$$\rho_{\mathrm{nf}}\left(u\frac{\partial v}{\partial x}+v\frac{\partial v}{\partial y}+w\frac{\partial v}{\partial z}\right)=-\frac{\partial p}{\partial y}+\mu_{\mathrm{nf}}\left(\frac{\partial^2 v}{\partial x^2}+\frac{\partial^2 v}{\partial y^2}+\frac{\partial^2 v}{\partial z^2}\right)+S_F(y) \tag{2}$$

$$\rho_{\mathrm{nf}}\left(u\frac{\partial w}{\partial x}+v\frac{\partial w}{\partial y}+w\frac{\partial w}{\partial z}\right)=-\frac{\partial p}{\partial z}+\mu_{\mathrm{nf}}\left(\frac{\partial^2 w}{\partial x^2}+\frac{\partial^2 w}{\partial y^2}+\frac{\partial^2 w}{\partial z^2}\right)+S_F(z). \tag{3}$$

Continuity equation:

$$\frac{\partial u}{\partial x}+\frac{\partial v}{\partial y}+\frac{\partial w}{\partial z}=0. \tag{4}$$

The energy equation is as follows:

$$(\rho_{\mathrm{m}}C_{\mathrm{p}})_{\mathrm{nf}}\left(u\frac{\partial T}{\partial x}+v\frac{\partial T}{\partial y}+w\frac{\partial T}{\partial z}\right)=k_{\mathrm{nf}}\left(\frac{\partial^2 T}{\partial x^2}+\frac{\partial^2 T}{\partial y^2}+\frac{\partial^2 T}{\partial z^2}\right)+S_E. \tag{5}$$

The terms $S_F(x)$, $S_F(y)$ and $S_F(z)$ are the momentum source terms and S_E is the energy source term caused by the presence of the magnetic field. These terms, resulting from the electric current of the wire, are the Kelvin force and can be calculated as follows [22]:

$$S_F(x)=\mu_0 M\frac{\partial H}{\partial x}\,,\qquad S_F(y)=\mu_0 M\frac{\partial H}{\partial y}\,,\qquad S_F(z)=\mu_0 M\frac{\partial H}{\partial z}\,. \tag{6}$$

Besides, the energy source term can be calculated by [22]

$$S_E=\frac{1}{\sigma_{\mathrm{nf}}}(\vec{J}\times\vec{J}),\qquad \vec{J}=\sigma_{\mathrm{nf}}(\vec{V}\times\vec{B}),\qquad \sigma_{\mathrm{nf}}=(1-\varphi)\cdot\sigma_{\mathrm{f}}+\varphi\cdot\sigma_{\mathrm{p}}. \tag{7}$$

It is obvious that the magnetic field (H) of the electric current is required. If the electric current was in the z-direction, the components of the magnetic field in the x- and y-directions are given by [22]

$$H_x(x,y)=\frac{I}{2\pi}\frac{(x-a)}{(x-a)^2+(y-b)^2} \tag{8}$$

$$H_y(x,y)=\frac{I}{2\pi}\frac{(y-b)}{(x-a)^2+(y-b)^2}\,. \tag{9}$$

The magnitude intensity of the magnetic field is defined as follows:

$$H(x,y,z)=\frac{I}{2\pi}\frac{1}{\sqrt{(x-a)^2+(y-b)^2}}\,. \tag{10}$$

Moreover, the terms B and M should be defined. The term B is the magnetic density flux which can be calculated by the intensity of magnetic field,

$$\vec{B}=\mu_0\times\mu_r\times H, \tag{11}$$

and M is the magnetization and is calculated as [23]

$$M=\frac{6m_{\mathrm{p}}}{\pi d_{\mathrm{p}}^3}\left[\coth(\xi)-\frac{1}{\xi}\right]\approx\frac{6m_{\mathrm{p}}}{\pi d_{\mathrm{p}}^3}[(\xi)/3]. \tag{12}$$

The magnetic moment for the particles is defined by

$$m_{\mathrm{p}}=\frac{4\mu_B\pi d_{\mathrm{p}}^3}{6\times 91.25\times 10^{-30}} \tag{13}$$

and ξ (Langevin parameter) is obtained by [23]

$$\xi=\frac{\mu_0 m_{\mathrm{p}}H}{k_BT}\,. \tag{14}$$

The dimensionless magnetic number (Mn) is used to evaluate the effect of the magnetic field intensity. The magnetic number (Mn) depends on the magnetic field intensity and is measured as follows:

$$Mn=\frac{\mu_0\chi H_r^2h^2}{\rho_{\mathrm{nf}}\alpha_{\mathrm{nf}}^2}\,, \tag{15}$$

where χ is the magnetic susceptibility of the nanofluid and is equal to M/H. Also, H_r is the characteristic of magnetic field strength and is obtained by $H_r=H(a,0)=\frac{I}{2\pi b}$.

The nanofluid physical properties can be obtained as follows.
Nanofluid density [24]:

$$\rho_{\mathrm{nf}} = (1-\varphi)\cdot\rho_{\mathrm{f}} + \varphi\cdot\rho_{\mathrm{p}}. \tag{16}$$

The heat capacity of the nanofluid is given by

$$C_{\mathrm{p_{nf}}} = \frac{(1-\varphi)(\rho c_{\mathrm{p}})_{\mathrm{f}} + \varphi(\rho c_{\mathrm{p}})_{\mathrm{p}}}{\rho_{\mathrm{nf}}}\,. \tag{17}$$

For the estimation of the effective viscosity of the nanofluid, the model proposed by Sundar *et al.* [25] has been utilized in this paper:

$$\mu_{\mathrm{nf}} = \mu_{\mathrm{f}}\left(1 + \frac{100\times\varphi}{12.5}\right)^{6.356}. \tag{18}$$

The effective thermal conductivity of the nanofluid is calculated by [26,27]

$$\frac{k_{\mathrm{nf}}}{k_{\mathrm{f}}} = 1 + 64.7\varphi^{0.746}\left(\frac{d_{\mathrm{f}}}{d_{\mathrm{p}}}\right)^{0.369}\left(\frac{k_{\mathrm{p}}}{k_{\mathrm{f}}}\right)^{0.7476} {Pr_{\mathrm{f}}}^{0.9955}{Re_{\mathrm{f}}}^{1.2321}, \tag{19}$$

where d_{f} and d_{p} are molecular diameter of the base fluid and the particle diameter, respectively. In eq. (19), the Pr_{f} and Re_{f} are defined as follows:

$$Pr_{\mathrm{f}} = \frac{\eta}{\rho_{\mathrm{f}}\alpha_{\mathrm{f}}}\,, \quad \eta = 2.414\times10^{-5}\times10^{\left(\frac{247}{T-140}\right)}$$
$$Re_{\mathrm{f}} = \frac{\rho k_B T}{3\pi\eta^2\lambda_{\mathrm{f}}}\,, \quad \lambda_{\mathrm{f}} = \text{Water mean free path} = 17\,\mathrm{nm} \text{ and } k_B = 1.3807\times10^{-23}\,\mathrm{J/K}.$$

The Reynolds number and Nusselt number of the system as main non-dimensional numbers are obtained as

$$Re_{\mathrm{nf}} = \frac{\rho_{\mathrm{nf}} v_{\mathrm{nf}} D}{\mu_{\mathrm{nf}}} \tag{20}$$

$$Nu(x) = \frac{h(x)\cdot D}{k_{\mathrm{nf}}}\,, \tag{21}$$

where $h(x)$ is the local convective heat transfer coefficient

$$h(x) = \frac{q''}{(T_w(x) - T_{\mathrm{f}}(x))}\,, \qquad T_{\mathrm{f}}(x) = T_{\mathrm{f}}(0) + \frac{q''\cdot P}{\dot{m}\cdot C_{\mathrm{p}}}x. \tag{22}$$

In the present study, the SIMPLEC algorithm is applied with the second-order upwind numerical scheme, and all the governing equations are solved through a finite volume CFD in-house code [28–35].

2.3 Boundary and flow conditions

The inflow conditions of the ferrofluid are equivalent to $Re_{\mathrm{m}} = 50$–200. In order to calculate the heat transfer, results of the Nusselt number have been presented for the water-based ferrofluid containing a wide range of spherical shape particles (0.86 to 4 vol% Fe_3O_4) with 60 nm mean diameter [21]. Inlet velocity with constant temperature ($T_{\mathrm{hot,in}} = T_0$) was applied to the ferrofluid inflow and a constant heat flux was applied for the tube wall ($q = 500$ to $2000\,\mathrm{W/m^2}$).

3 Results

3.1 Validation

In the first step, our numerical simulations are compared with Azizian *et al.* [21] experimental test runs. In order to preserve a similar operating condition, the Nusselt number of water along the pipe at constant velocity is studied. In this model, the wall of the pipe is under a constant heat flux ($q = 1000\,\mathrm{W\,m^{-2}}$). Figure 3(b) compares the Nusselt number of the numerical simulation with the experimental data of Azizian *et al.* [21] along the tube for two inlet velocities. The comparison shows that the numerical results present good agreement with experimental results.

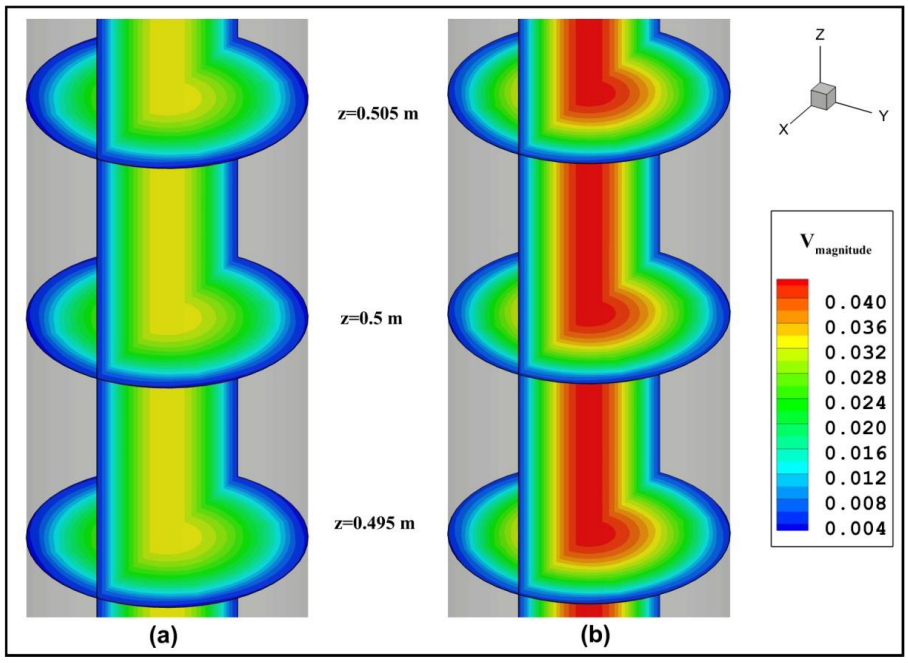

Fig. 4. Comparison of the velocity of the flow inside the tube ($Re = 100$) (a) without nanoparticles and (b) with nanoparticles.

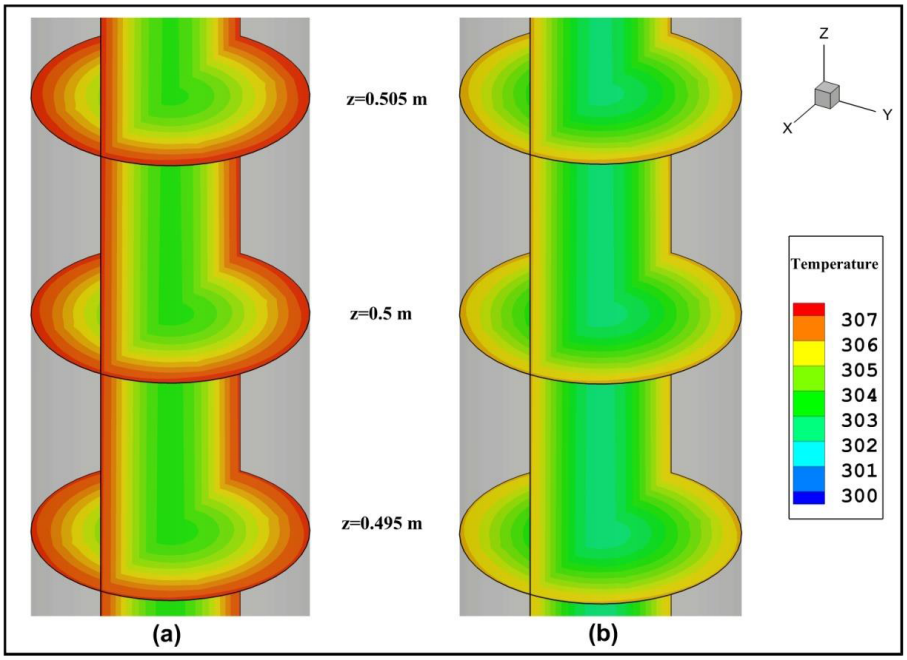

Fig. 5. Comparison of the temperature distribution of the flow inside the tube ($Re = 100$) (a) without nanoparticles and (b) with nanoparticles.

3.2 Flow characteristic of nanofluid inside the tube

Figure 4 compares the velocity of the magnitude inside the tube for water with/without nanoparticles. The contour clearly shows that the maximum velocity at the center of the tube increases when nanoparticles are added to the base fluid at constant Reynolds number ($Re = 100$). According to empirical correlations of Sundar *et al.* [24], the viscosity of the fluid significantly increases when nanoparticles are present in the base fluid. Hence, the velocity of the fluid rises in the core of the tube at constant Reynolds number. Moreover, the gradient of the velocity profile is increased by increasing of fluid viscosity.

Figure 5 illustrates the temperature distribution inside the tube in various cross sections. The results show that the temperature variation decreases in the tube with nanofluids. As water is replaced by nanofluids, the viscosity increases by about 36% ($\mu_{\text{water}} = 0.00096$ and $\mu_{\text{nano-0.86\%}} = 0.00131$) while the density rises by about 3% ($\rho_{\text{water}} = 997$ and $\rho_{\text{nano-0.86\%}} = 1033$). Therefore, the nanofluid should have a higher inlet velocity at constant Reynolds number.

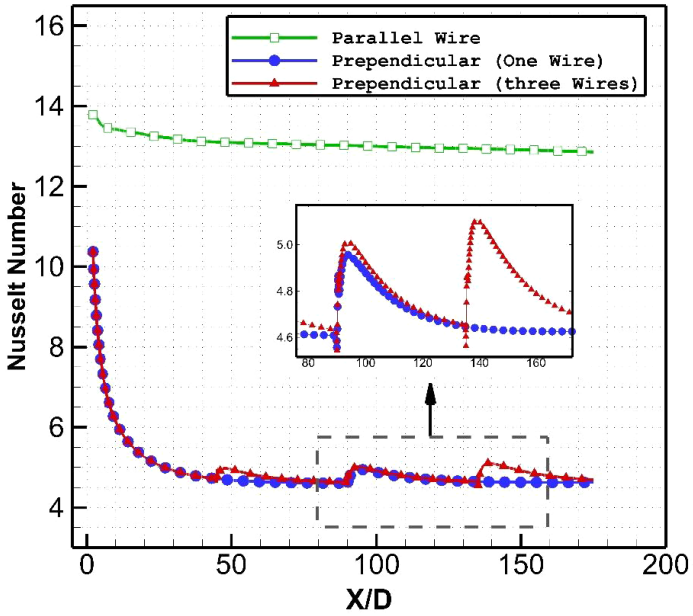

Fig. 6. Effect of the wire orientation on the heat transfer along the tube. (The position of the wire is 0.25, 0.5 and 0.75 m for three perpendicular wires.)

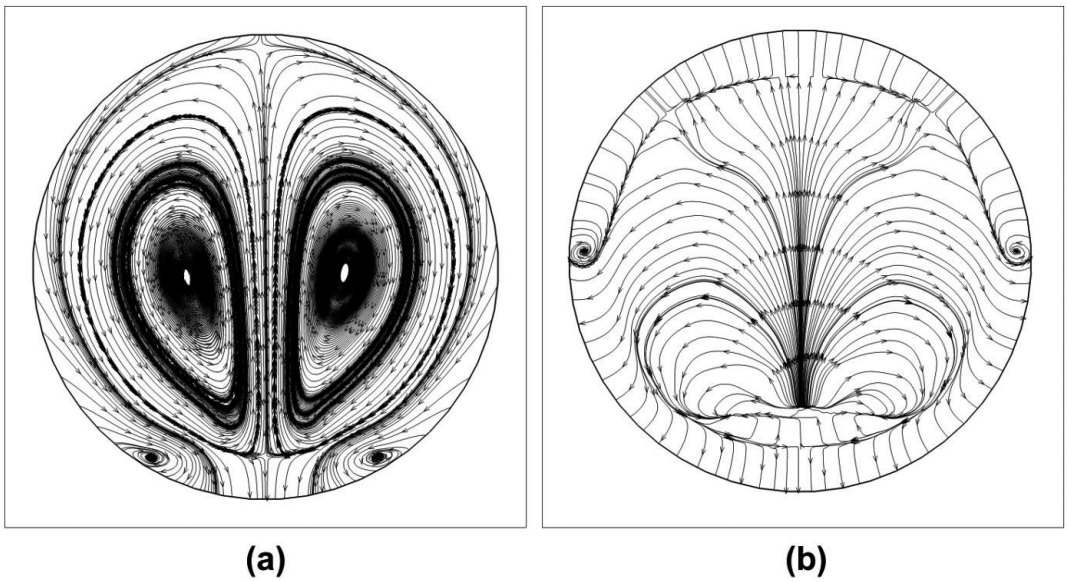

Fig. 7. Comparison of the stream function on the x-y plane in the middle of the tube ($Re = 100$) in the presence (a) of a parallel wire and (b) of a perpendicular wire.

(For $Re = 100$ we have $U_{\text{water}} = 0.017$ and $U_{\text{nano-0.86\%}} = 0.023$.) With increasing the nanofluid velocity, the mass flow rate of the fluid rises in the tube. Thus, heat transfer enhances in the fluid and temperature decreases in the domain.

3.3 The influence of wire orientation

In this section, the effects of different orientations of the wire as a source of magnetic field on the heat transfer of the ferrofluid are examined. In addition, the influence of three perpendicular wires on heat transfer are investigated. Figure 6 illustrates the Nusselt number along the tube in three different wire arrangements. The comparison clearly shows that the parallel wire presents a significantly higher heat rate in the tube. As was expected, the presence of three wires with the perpendicular orientation enhances the heat transfer in the local area in the vicinity of the wire. However, the value of this increase is subtle in comparison with the parallel wire.

In order to inspect the effects of the magnetic field on the flow feature, the stream function of the flow in the middle of the tube is compared in fig. 7. The parallel wire yields a non-uniform magnetic field in the x- and y-directions. This field is perpendicular to the ferrofliud flow direction. The presence of a magnetic field induces the force to flow in cross planes. This results in a secondary flow, which appears as two eddies.

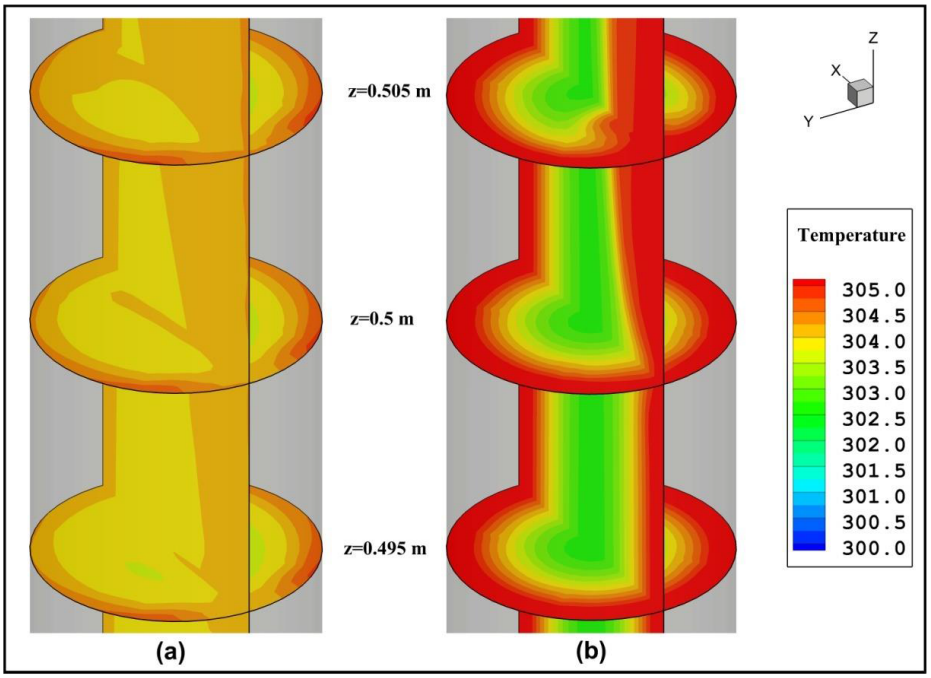

Fig. 8. Effect of wire orientation on the temperature distribution inside the tube ($Re = 100$) in the presence (a) of a parallel wire and (b) of a perpendicular wire (the wire is located in the $z = 0.5$ direction).

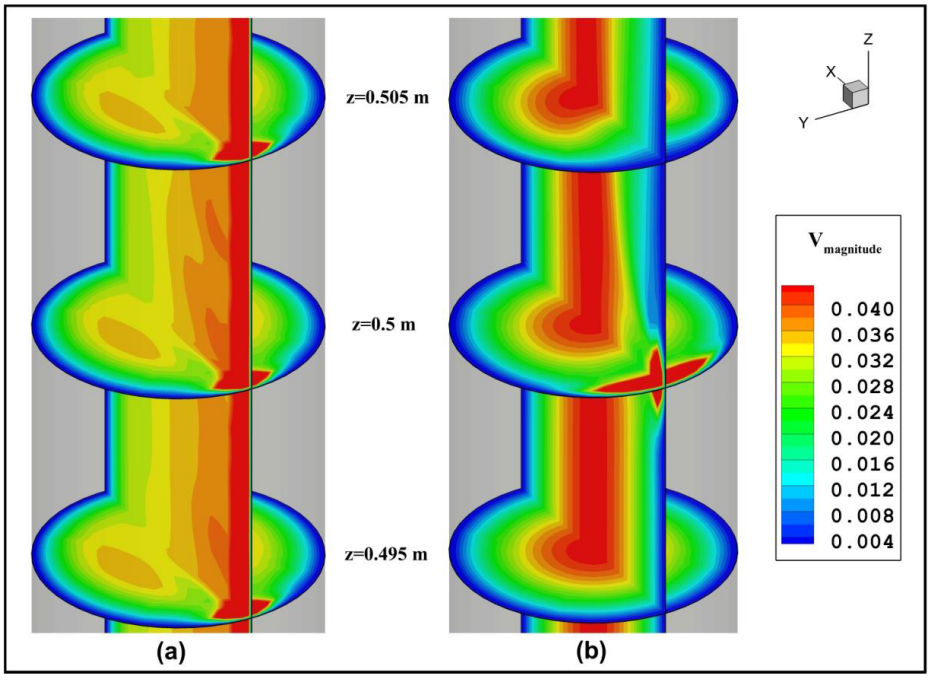

Fig. 9. Effect of wire orientation on the average velocity inside the tube ($Re = 100$) in the presence (a) of a parallel wire and (b) of a perpendicular wire.

For the parallel wire (fig. 7(a)), two strong eddies are formed in the section. On the other side, two weak eddies are observed in the section of the tube when the orientation of the wire is perpendicular to the axis of the tube. Figures 8 and 9 show the contour of temperature and velocity along the tube in the parallel and perpendicular orientations of the wire, respectively. Figure 8 (temperature distribution) shows that the temperature reduces in the tube with parallel wire. Figure 9 (velocity contour) clearly indicates that the velocity increases in the vicinity of the wire due to the high magnetic field. According to both temperature and velocity contours, the flow feature forms a three-dimensional profile with strong eddies when the wire is parallel to the tube axis. It is also found that the strong eddy has significant influences on the heat transfer of the flow. Since the influence of the perpendicular wire is not noticeable in the heat transfer rate, the parallel wire is chosen as the main source of magnetic field in the following sections.

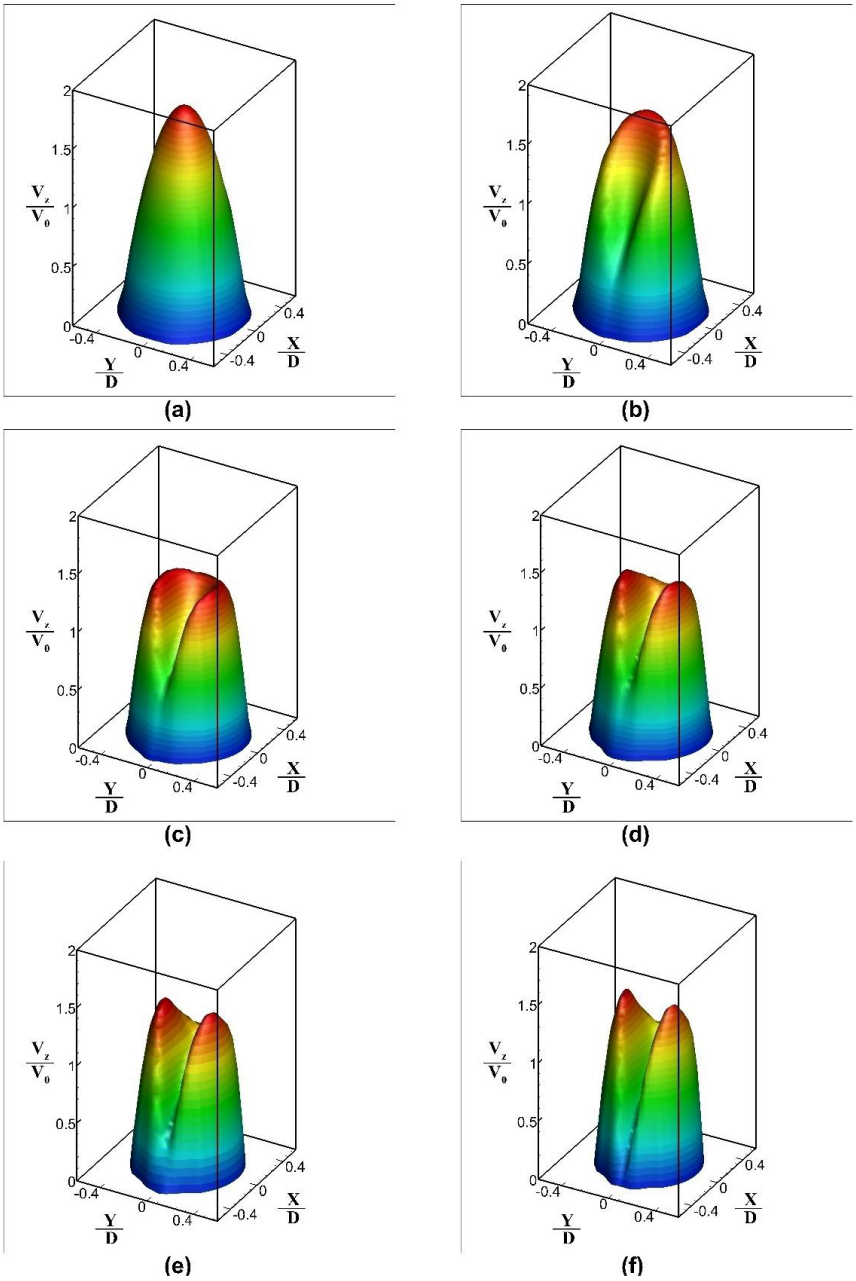

Fig. 10. Comparison of the z-velocity on the plane in the middle of tube ($Re = 100$) for various magnetic fields: (a) $Mn = 0$; (b) $Mn = 4.69e + 7$; (c) $Mn = 1.88e + 8$; (d) $Mn = 4.22e + 8$; (e) $Mn = 7.5e + 8$; (f) $Mn = 1.17e + 9$.

3.4 Parametric study

Figure 10 shows the z-velocity profile of the nanofluid on the plane in the middle of the tube under different magnetic numbers. It can be seen that a non-uniform magnetic field changes the velocity gradient near the wall and strengthens two eddies inside the tube. In fact, these eddies lead to the formation of a secondary flow in the x-y plane. Two eddies are symmetric with respect to the y-axis. It can be seen that streamlines recede from electrical wire as a result of Kelvin force.

Figure 11 shows the variation of the Nusselt number along the axis of the tube in the presence of different magnetic field intensities. The plot shows that the heat transfer meaningfully increases when a non-uniform magnetic field is applied to the tube. The variation of the Nusselt number for the various magnetic field intensities indicates that the average heat transfer rate does not change noticeably by increasing the magnetic field intensity at high magnetic numbers. The variations of the Nusselts number show that the rate of the heat transfer increases along the x-direction.

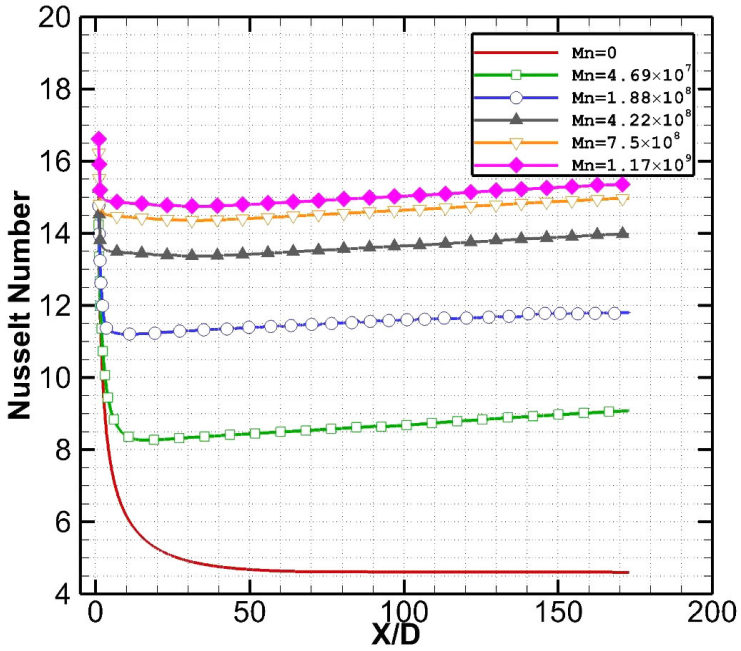

Fig. 11. The effect of various magnetic intensities on the Nusselt number along the tube axis ($Re = 100$).

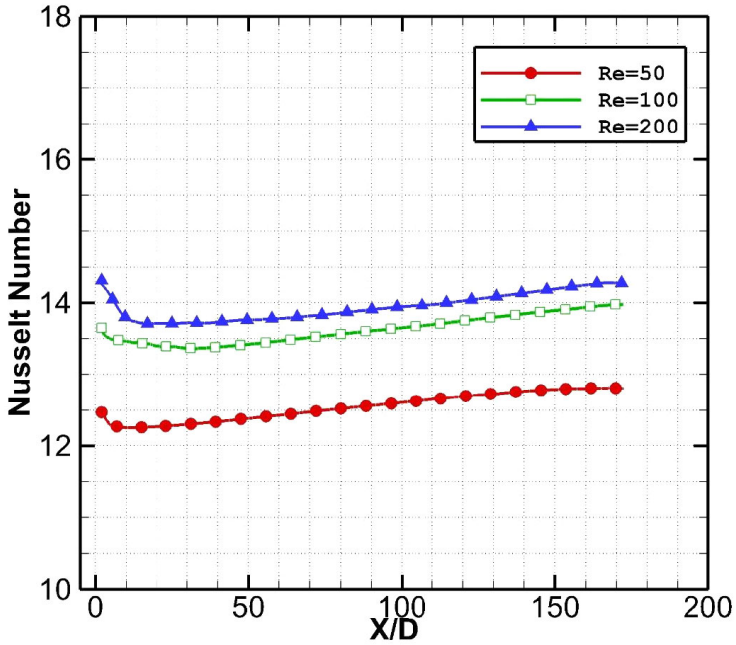

Fig. 12. Variation of the Nusselt number along the tube for different inlet velocities ($Mn = 4.22e + 8$).

This is due to the increase in the fluid temperature along the streamwise direction. Therefore, the properties of the nanofluid are varied and this makes the heat transfer of the tube increase.

Figure 12 illustrates the variation of the Nusselt number along the tube for the various inlet velocities ($Re = 50$, 100 and 200) under constant magnetic field ($Mn = 4.22e + 8$). As mentioned earlier, the Nusselts number increases along the axis of the tube due to the change in the fluid properties. As is shown in the figure, the increase in the Reynolds number is not directly proportional to that of the Nusselts number. Figure 13 shows the temperature distribution on the section in the middle of the tube. The comparison shows that the temperature of the core of the eddy decreases when the Reynolds number is increased. As the Reynolds number increases, the temperature gradient intensifies in the vicinity of the wall. Indeed, this occurs due to the high heat transfer.

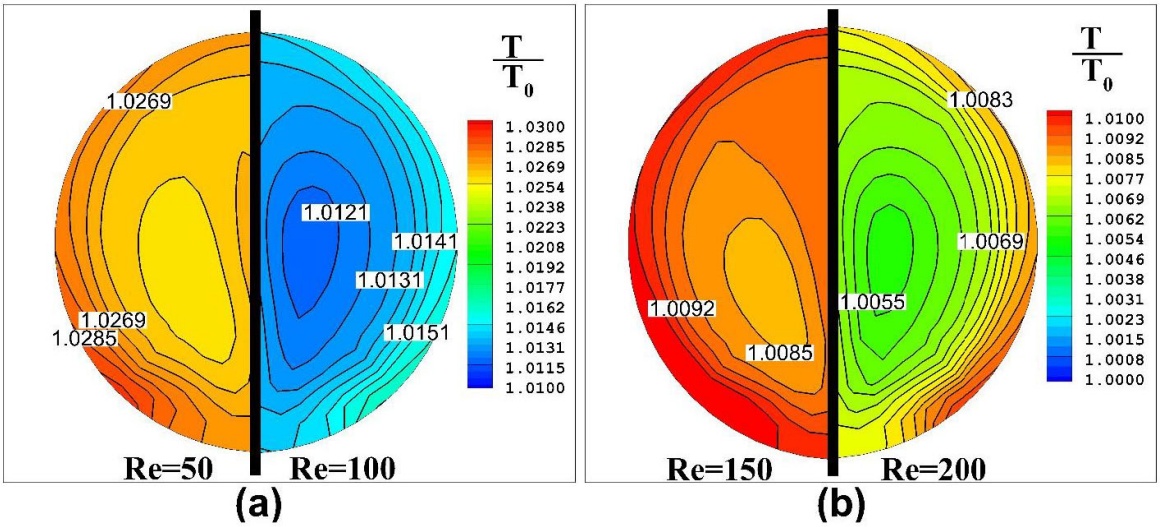

Fig. 13. Comparison of non-dimensional temperature on the plane in the middle of the tube ($Mn = 4.22e+8$). It is noted that the range of each figure ((a) and (b)) is not the same.

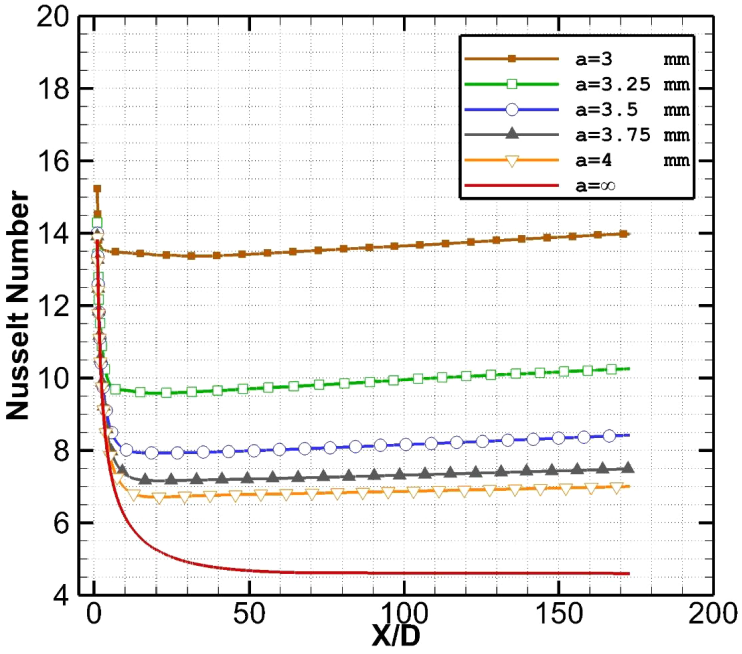

Fig. 14. The effect of the wire distance to tube on the heat transfer (Nusselt number) along the tube ($Re = 100$, $Mn = 4.22e+8$).

Figure 14 plots the effects of the wire distance to the tube on the heat transfer (Nusselt number) for $Re = 100$, $Mn = 4.22e + 8$. The figure clearly shows that the heat transfer substantially increases when the wire gets closer to the tube. In fact, the effect of the magnetic field intensifies exponentially in the normal direction. The results confirm that the heat transfer increases along the tube because of the change in the properties of the ferrofluid inside the tube.

The effect of nanoparticle concentration on the average Nusselt number along the axis of the tube is presented in fig. 15 for $Re = 100$. As expected, with an increase in nanoparticles, the averaged Nusselt number intensifies due to the effects of the magnetic field on the nanoparticles.

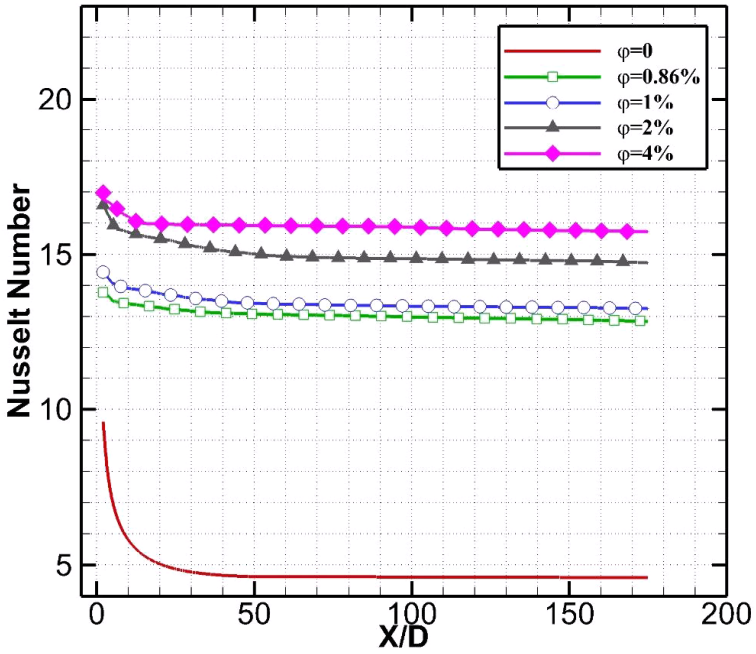

Fig. 15. Variation of the Nusselt number along the tube for various concentrations of nanoparticles ($Re = 100$).

4 Conclusion

In this article, a numerical investigation was performed on the nanofluid magnetic flow in a tube under non-uniform magnetic field. In the first step, the temperature distribution and hydrodynamic features of the nanofluid are compared with those of the base fluid. The obtained results show that the presence of nanoparticles significantly enhances the heat transfer in the tube. Then, the effects of the magnetic field on the heat transfer of the nanofluid inside the tube is investigated. The influence of various orientations of the magnetic field is examined. Our findings show that the Nusselt number increases by more than 300 percent in the presence of magnetic field. In addition, the hydrodynamic feature of the nanofluid is comprehensively discussed. The effects of various parameters, such as magnetic intensity, particle concentration and distance of the magnetic field, are also studied. According to our results, the presence of the magnetic field considerably intensifies the heat transfer when the wire as the source of the non-uniform magnetic field is in a parallel orientation with the axis of the tube.

References

1. M.B. Gerdroodbary, M.R. Takami, D.D. Ganji, Case Stud. Thermal Eng. **6**, 28 (2015).
2. B. Mahanthesh, B.J. Gireesha, Alex. Eng. J. **55**, 569 (2016).
3. Ahmed Kadhim Hussein, M.A.Y. Bakier, Mohamed Bechir Ben Hamida, S. Sivasankaran, Alex. Eng. J. **55**, 2157 (2016).
4. Dongsheng Wen, Guiping Lin, Saeid Vafaei, Kai Zhang, Particuology **7**, 141 (2009).
5. I. Behroyan, Sh.M. Vanaki, P. Ganesan, R. Saidur, Int. Commun. Heat Mass Transfer **70**, 27 (2015).
6. Mohsen Sheikholeslami, Mofid Gorji Bandpy, Hamid Reza Ashorynejad, Physica A **432**, 58 (2015).
7. Ningbo Zhao, Jialong Yang, Hui Li, Ziyin Zhang, Shuying Li, Int. J. Heat Mass Transfer **92**, 268 (2016).
8. Mohsen Sheikholeslami, Davood Domiri Ganji, Physica A **417**, 273 (2015).
9. S. Valiallah Mousavi, M. Sheikholeslami, Mofid Gorji bandpy, M. Barzegar Gerdroodbary, Chem. Eng. Res. Des. **113**, 112 (2016).
10. S.V. Mousavi, M.B. Gerdroodbary, M. Sheikholeslami, D.D. Ganji, Eur. Phys. J. Plus **131**, 347 (2016).
11. M. Sheikholeslami, D.D. Ganji, J. Taiwan Inst. Chem. Eng. **65**, 43 (2016).
12. Doohyun Kim, Younghwan Kwon, Yonghyeon Cho, Chengguo Li, Seongir Cheong a, Yujin Hwang, Jaekeun Lee, Daeseung Hong, Seongyong Moon, Curr. Appl. Phys. **9**, 119 (2009).
13. M. Sheikholeslami, M.M. Rashidi, T. Hayat, D.D. Ganji, J. Mol. Liq. **218**, 393 (2016).
14. A. Abdollahi, M.R. Salimpour, Eur. Phys. J. Plus **131**, 41 (2016).
15. A. Abdollahi, M.R. Salimpour, N. Etesami, Appl. Therm. Eng. **111**, 1101 (2017).
16. Hussein Togun, H.I. Abu-Mulaweh, S.N. Kazi, A. Badarudin, Int. Commun. Heat Mass Transfer **71**, 108 (2016).
17. M. Sheikholeslami, M.B. Gerdroodbary, D.D. Ganji, Comput. Methods Appl. Mech. Eng. **315**, 831 (2017).

18. M. Hatami, S.A.R. Sahebi, A. Majidian, M. Sheikholeslami, D. Jing, G. Domairry, J. Mol. Liq. **212**, 785 (2015).
19. M. Sheikholeslami, M. Hatami, D.D. Ganji, J. Mol. Liq. **211**, 577 (2015).
20. Mohammad Goharkhah, Mehdi Ashjaee, Mahmoud Shahabadi, Int. J. Therm. Sci. **99**, 113 (2016).
21. R. Azizian, E. Doroodchi, T. McKrell, J. Buongiorno, L.W. Hu, B. Moghtaderi, Int. J. Heat Mass Transfer **68**, 94 (2014).
22. M. Nasiri, M.M. Rashidi, G. Lorenzini, Entropy **18**, 10 (2016).
23. H. Yamaguchi, *Engineering Fluid Mechanics* (Springer Science, Netherlands, 2008).
24. B.C. Pak, Y.I. Cho, Exp. Heat Transf. **11**, 151 (1998).
25. L.S. Sundar, K.V. Sharma, M.T. Naik, M.K. Singh, Renew. Sustain. Energy Rev. **25**, 670 (2013).
26. R.L. Hamilton, O.K. Crosser, Industr. Eng. Chem. Fund. **1**, 187 (1962).
27. K.H.J. Buschow, *Handbook of Magnetic Materials* (Elsevier, 2003).
28. M.B. Gerdroodbary, M. Mokhtari, S. Bishehsari, K. Fallah, Asian J. Atmos. Environ. **10**, 125 (2016).
29. M.B. Gerdroodbary, M. Mokhtari, K. Fallah, H. Pourmirzaagha, Int. J. Hydrogen Energy **41**, 22497 (2016).
30. Y. Amini, M. Mokhtari, M. Haghshenasfard, M.B. Gerdroodbary, Case Stud. Therm. Eng. **6**, 104 (2015).
31. M. Mokhtari, M.B. Gerdroodbary, R. Yeganeh, K. Fallah, Eng. Sci. Technol. (2016) DOI:10.1016/j.jestch.2016.12.007.
32. M. Barzegar Gerdroodbary, O. Jahanian, M. Mokhtari, Int. J. Hydrogen Energy **40**, 9590 (2015).
33. M.B. Gerdroodbary, M.R. Takami, H.R. Heidari, K. Fallah, D.D. Ganji, Acta Astron. **123**, 283 (2016).
34. M.B. Gerdroodbary, D.D. Ganji, Y. Amini, Acta Astron. **115**, 422 (2015).
35. M.B. Gerdroodbary, K. Fallah, H. Pourmirzaagha, Acta Astron. **132**, 25 (2017).